[redacted]

Navy Department - Office of Research and Inventions

FR-2863

NAVAL RESEARCH LABORATORY
Washington, D. C.

MECHANICS AND ELECTRICITY DIVISION - BALLISTICS SECTION

15 June 1946

PRELIMINARY REPORT ON DYNAMIC PENETRATION BY CONES

by

A. J. Hodges, G. R. Irwin
and J. R. Streeter

-Report 0-2863-

[redacted]

* UNCLASSIFIED *

Approved by:

. Ross Gunn, Superintendent
chanics & Electricity Division

Commodore H. A. Schade, USN
Director, Naval Research Laboratory

Preliminary Pages... a-c
Numbered Pages..... 29
Tables 16
Plates..... 12
Distribution List... d

DISTRIBUTION STATEMENT A APPLIES
Further distribution authorized by: ---
UNLIMITED only.

NRL Problem O-62

[redacted]

Navy Department - Office of Research and Inventions

NAVAL RESEARCH LABORATORY
Washington, D. C.

MECHANICS AND ELECTRICITY DIVISION - BALLISTICS SECTION

15 June 1946

PRELIMINARY REPORT ON DYNAMIC PENETRATION BY CONES

by

A. J. Hodges, G. R. Irwin
and J. R. Streeter

-Report O-2863-

[redacted]

* * *

Approved by:

Dr. Ross Gunn, Superintendent
Mechanics & Electricity Division

Commodore H. A. Schade, USN
Director, Naval Research Laboratory

Preliminary Pages... a-c
Numbered Pages..... 29
Tables 16
Plates..... 12
Distribution List... d

NRL Problem O-62

ABSTRACT

Studies have been made of deceleration of cone-headed projectiles in the entry phase of penetration at velocities of 600 to 2400 ft/sec. The theoretical considerations underlying this method for studying velocity effects in penetration resistance are discussed. Methods of handling the data to obtain numerical values for the velocity term and the term dependent on strain rate are discussed and illustrated. It is shown that the more reliable data obtained, ranging from 2×10^4 to 24×10^4 $(sec)^{-1}$ straining speed, are well represented by a formula for deformation pressure which consists of three additive terms: (1) a velocity independent "constant pressure" term, (2) a term proportional to straining speed (velocity to depth ratio), (3) a term proportional to the product of displaced volume times energy of motion of the penetrator.

It is also shown that lubrication effects must be considered in studies of this nature.

With improved measurement techniques the procedures described in this report should give good quantitive measurements of strain rate and velocity effects in a rapid penetration process simplified enough for general use of the results.

TABLE OF CONTENTS

[redacted]

AUTHORIZATION AND INTRODUCTION

1. The study of penetration dynamics was authorized by BuOrd. Project Order No. E-4840.

2. The influence of physical properties of materials upon their resistance to dynamic penetration has been considered in the past only under circumstances where the complexities of the deformation process made a semi-empirical approach necessary. Substantial progress in the understanding of the many complexities of penetration dynamics can not be made until careful examination and analysis have been carried out under other simplified conditions of impact.

3. When the penetration is of the class in which material displaced by the penetrator is principally pushed aside rather than projected as a punching, the expectations are that (a) there will be a rough correlation between indentation hardness and overall penetration resistance, and (b) the resisting force components which depend on velocity and strain rate are (at velocities below 2800 ft/sec) generally small compared to those which depend only on shape and on physical properties for slow speed deformation. To this class of penetrations belong the cone indents discussed in this report.

4. The use of conical penetrators as discussed in this report provides sufficient simplicity in the pattern of material deformation so that hypotheses regarding velocity and strain rate effects can be investigated with a minimum of ambiguity. During the penetration of a cone, there exists approximate similitude of the geometry of deformation of the penetrated material; that is, for successive positions of the cone the ratio of the dimensions of the indentations to one another remains constant.

Because of similitude, indentations of various depths may be compared as long as the cone angles are the same.

5. Two important justifications for an investigation of conical penetrations are as follows:

a. The cone indentations can be interpreted as similar to certain phases of penetration by more complex ogival shapes thus leading to the development of an improved theory of projectile penetration.

b. An understanding of the tendencies toward brittle fracture will be aided by an investigation of strain rate effects upon resistance and, particularly, if sufficient precision can be obtained, of differences between materials in a range of very short relaxation times.

6. This report is intended primarily as a description of an experimental method with enough interpretation of results to illustrate the application to penetration theory. Since the collection of data presented in this report, certain modifications of apparatus permitting greater precision have been made, and others are being developed. The theoretical considerations likewise cannot be presented in more than a preliminary form at the present time.

7. Included in this study were experiments on lubrication effects. Earlier studies (reference 1) had shown marked lubrication effects in dynamic indentations in plastics. Information about recent lubricants used for bearings moving at high speeds under heavy loads led to preliminary trials of molybdenum sulfide and stearic acid. Stearic acid proved to be the better lubricant, and comparisons were made between the poorest

condition of lubrication that could be achieved and that of stearic acid coated cones and that of oil coated cones.

THEORETICAL BACKGROUND

8. There is a class of penetration phenomena in which the penetrator, like a torpedo moving along steadily under water or a projectile piercing a very thick metal plate, is continuously activating similar patterns of flow in a previously undisturbed portion of the penetrated medium without increase in deformation resistance as the path length increases. On the other hand in cone penetrations, until the rim of the cone head bears against plate material, the penetration is always in the entry phase. If the plate is thick and cavitation effects may be neglected, then, approximately, the flow pattern at any instant is a larger size model of the flow pattern at any preceding instant.

9. With respect to energy of translation of moving plate material it is clear that the volume-elements for similar sections of flow pattern are in proportion to the total displaced volume of plate material at the instant in question. Consider the impact as occurring at the origin of a rectangular x, y, z coordinate system with the axis of the cone along the z-axis and the face of the plate in the $z = 0$ plane. Let s be the z displacement of the point of the cone. Let $d\omega$ be any small volume element of moving plate material and du be its translational displacement in time dt. Then the element $d\omega$ has energy of translation equal to

$$\frac{1}{2}\rho\, d\omega \left(\frac{du}{dt}\right)^2 \qquad \text{or} \qquad \frac{1}{2}\rho\, d\omega \left(\frac{du}{ds}\right)^2 \left(\frac{ds}{dt}\right)^2.$$

Thus the total energy of translation of plate material, T.E., is the integral

[redacted]

$$T.E. = \frac{1}{2}\rho \left(\frac{ds}{dt}\right)^2 \int \left(\frac{du}{ds}\right)^2 d\omega \qquad (1)$$

where ρ is the density of the plate material. Writing v for $\left(\frac{ds}{dt}\right)$ and using the symbol Ω for total volume of plate material displaced by the penetrator we have

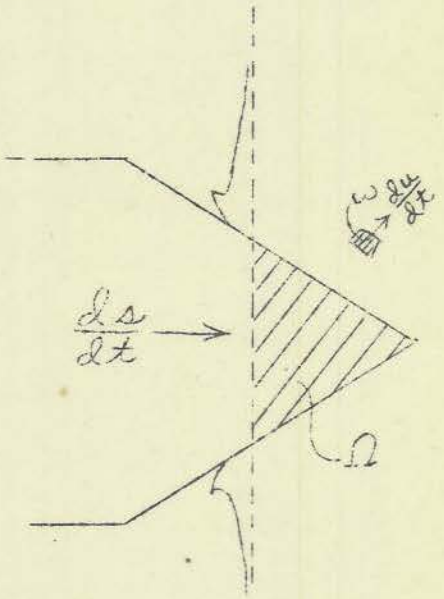

$$T.E. = \frac{1}{2}\rho v^2 \Omega \int \left(\frac{du}{ds}\right)^2 \frac{d\omega}{\Omega} \qquad (2)$$

It is clear from the similitude considerations discussed above that the above integral is very approximately independent of velocity and depth of indentation.

If we put

$$\alpha = \int \left(\frac{du}{ds}\right)^2 \frac{d\omega}{\Omega} \qquad (3)$$

then

$$T.E. = \frac{1}{2}\alpha\rho v^2 \Omega = \frac{\alpha\rho}{m} E \Omega \qquad (4)$$

where m is the mass and E the kinetic energy of the penetrator. The contribution of this effect to force per unit area on the penetrator is

$$\frac{\partial(T.E.)}{\partial \Omega} = \frac{\alpha\rho}{m} E + \frac{\alpha\rho}{m} \Omega \frac{\partial E}{\partial \Omega} \qquad (5)$$

The first term is the familiar Poncelet type velocity effect term. The second term is properly small or absent in the deep, head embedded type of penetration but must be retained in the analysis of results for the cone entry studies of this report. The calculation of α from theoretical considerations while not included in this report has at least been greatly simplified over penetrations with ogival head shape. It is clear that $\left(\frac{\partial u}{\partial s}\right)^2$ decreases rapidly as distance from the surface of the penetrator increases and can in no case exceed unity. The integral of $\frac{\partial \omega}{\Omega}$ over those portions which have significant $\left(\frac{\partial u}{\partial s}\right)^2$ values would be a quantity of the order of unity. On may conclude that α is of the order of, but substantially less than, unity and that α will

vary with cone angle.

10. The contribution to resisting forces of strain rate effects is more complex. Consider the movement of any volume element of plate material, $d\omega$, resolved into translation, rotation, and certain shears. The contribution of rotational motion to velocity dependent resistance will be, like translation, proportional to $\frac{d(E\Omega)}{d\Omega}$ The contribution of rotation is a small term in the theoretical calculation of α and does not require separate discussion here. Consider the work done within $d\omega$ in an increase of a certain shear from θ to $(\theta + d\theta)$. If it is permissable to represent the torque resisting this shear as the product $\left[a_o + g\left(\frac{d\theta}{dt}\right)\right] \phi(\theta)$ then the small element of work done is

$$\left[a_o + g\left(\frac{d\theta}{dt}\right)\right] \phi(\theta)\, d\theta\, d\omega$$

$$= \left[a_o + g\left(\frac{d\theta}{dt}\right)\right] \cdot \phi(\theta) \left(s \frac{d\theta}{ds}\right) \frac{d\omega}{3\Omega}\, d\Omega \qquad (6)$$

It will be seen that if all such contributions are summed up throughout the deforming plate material there will be in the result a strain rate independent portion as follows:

$$a_o d\Omega \int \phi(\theta) \left(s \frac{d\theta}{ds}\right) \frac{d\omega}{3\Omega} = P\, d\Omega \qquad (7)$$

where P, because of the approximate similitude of the flow pattern at each instant, is independent of Ω, v, and $\left(\frac{d\theta}{dt}\right)$

11. Various hypotheses might be made as to the proper functional form for $g\left(\frac{d\theta}{dt}\right)$ as used above. A review of the literature, although disclosing interesting possibilities for organizing studies of strain rate effects under the relaxation times viewpoint, does not at present furnish any preferred choice. The hypothesis might be made for tentative consideration and trial that the term $g\left(\frac{d\theta}{dt}\right)$ is merely directly proportional to some power of the strain rate, that is

$$g\left(\frac{d\theta}{dt}\right) = a_r\left(\frac{d\theta}{dt}\right)^r = a_r\left(\frac{v}{s}\right)^r \left(s\,\frac{d\theta}{ds}\right)^r \qquad (8)$$

where a_r is a constant. The summing up of strain rate dependent contributions to work done throughout the deforming plate material then becomes

$$\int g\left(\frac{d\theta}{dt}\right)\phi(\theta)\left(s\,\frac{d\theta}{ds}\right)\frac{d\omega}{3\Omega}\,d\Omega$$

$$= a_r\left(\frac{v}{s}\right)^r d\Omega \int \phi(\theta)\left(s\,\frac{d\theta}{ds}\right)^{r+1}\frac{d\omega}{3\,d\Omega}$$

$$= b_r\left(\frac{v}{s}\right)^r d\Omega \qquad (9)$$

The quantity b_r like P is independent of Ω, v and $\left(\frac{d\theta}{dt}\right)$. The term $\frac{v}{s}$ will be called the "straining speed" hereafter. Note that straining speed is not the same thing as strain rate, but that it is a function of the strain rate and the geometry of flow of the plate material. The case, $r = 1$, is of some special interest because this may be considered the first term in a $\left(\frac{d\theta}{dt}\right)$

power series expansion of $g\left(\frac{d\theta}{dt}\right)$. We may note that if all terms of a $\left(\frac{d\theta}{dt}\right)$ power series for $g\left(\frac{d\theta}{dt}\right)$ were included the result would be

$$\int g\left(\frac{d\theta}{dt}\right) \cdot \phi(\theta) \cdot \left(s \frac{d\theta}{ds}\right) \frac{d\omega}{d\Omega} \, d\Omega$$

$$= d\Omega \sum_{r=1}^{\infty} b_r \left(\frac{v}{s}\right)^r = f\left(\frac{v}{s}\right) d\Omega \qquad (10)$$

Where each coefficient b_r depends in a different way upon the geometry of flow in the deforming plate material.

12. In the preceding paragraphs it has been shown that the cone headed penetrator experiences resisting forces which are such that the changes, $-dE$, in energy of motion of the penetrator may be represented as follows:

$$-dE = P d\Omega + f\left(\frac{v}{s}\right) \cdot d\Omega + \frac{d\rho}{m} \cdot \frac{d(\Omega E)}{d\Omega} d\Omega \qquad (11)$$

ANALYTICAL PROCEDURE

13. Equation (11) may be written as:

$$-\frac{dE}{d\Omega} = P + f\left(\frac{v}{s}\right) + \frac{d\rho}{m} \frac{d(\Omega E)}{d\Omega} \qquad (12)$$

but for a cone,

$$-\frac{dE}{d\Omega} = -\frac{m v dv}{k s^2 ds} = \frac{m}{k s^2} \frac{dv}{dt} = \frac{F}{A} \qquad (13)$$

[redacted]

where F is the force resisting penetration and A is the projected area of the indentation. Thus,

$$\frac{F}{A} = P + f\left(\frac{v}{s}\right) + \frac{\alpha\rho}{m} E - \frac{\alpha\rho}{m} \Omega \frac{F}{A} \qquad (14)$$

$$= P + f\left(\frac{v}{s}\right) + \frac{\alpha\rho}{m}\left(E - \frac{sF}{3}\right) \qquad (15)$$

By plotting $\frac{F}{A}$ against $\frac{v}{s}$ for a number of impacts, and choosing $\frac{F}{A}$ values at a constant value of $\frac{v}{s}$, one can plot $\left(\frac{F}{A}\right)_{\frac{v}{s}=c}$ against corresponding values of $\frac{\rho}{m}\left(E - \frac{sF}{3}\right)$. If the plot can be represented by a straight line, the slope of that line is α. Having evaluated α, one can examine the function $f\left(\frac{v}{s}\right)$ by plotting $\frac{F}{A} - \frac{\alpha\rho}{m}\left(E - \frac{sF}{3}\right)$ against $\frac{v}{s}$. Should $\frac{F}{A} - \frac{\alpha\rho}{m}\left(E - \frac{sF}{3}\right)$ be a linear function of $\frac{v}{s}$, one can write equation (11) as:

$$-dE = P\,d\Omega + b\,\frac{v}{s}\,d\Omega + \frac{\alpha\rho}{m}\,d(\Omega E) \qquad (16)$$

For a cone of angle γ

$$\frac{d\Omega}{ds} = \pi s^2 \tan^2\frac{\gamma}{2} = k s^2 \qquad (17)$$

Thus

$$\frac{v}{s}\, d\Omega = k\, v\, s\, ds \qquad (18)$$

and

$$-dE = P\, d\Omega + b k\, v\, s\, ds + \frac{\alpha\rho}{m}\, d(\Omega E) \qquad (19)$$

14. Integration gives

$$E_o - E = P\Omega + \frac{\alpha\rho}{m}\Omega E + b k \int v\, s\, ds \qquad (20)$$

$$\frac{E_o - E}{\Omega} = P + \frac{\alpha\rho}{m} E + \frac{b k}{\Omega} \int v\, s\, ds \qquad (21)$$

The term $\frac{k}{\Omega}\int v\, s\, ds$ can be graphically integrated. By plotting $\frac{E_o - E}{\Omega}$ against $\frac{k}{\Omega}\int v\, s\, ds$, one can select $\frac{E_o - E}{\Omega}$ values at the same value of $\frac{k}{\Omega}\int v\, s\, ds$, and plotting of these $\frac{E_o - E}{\Omega}$ values against corresponding values of $\frac{\rho E}{m}$ should give a straight line, the slope of which would be α. With evaluation of α, one can plot $\frac{E_o - E}{\Omega} - \frac{\alpha\rho}{m} E$ against $\frac{k}{\Omega}\int v\, s\, ds$. The slope of a linear plot is b, and the intercept is P

15. With evaluation of α, b, and P, one can calculate resistance values from values of v and s data by use of equation (14) as follows:

$$\frac{F}{A} + \frac{\alpha\rho}{m}\Omega\frac{F}{A} = P + b\frac{v}{s} + \frac{\alpha\rho}{m} E$$

$$\frac{F}{A} = \frac{1}{1 + \frac{\alpha\rho}{m}\Omega}\left[P + b\frac{v}{s} + \frac{\alpha\rho}{m} E\right] \qquad (22)$$

and the force equation is

$$F = \frac{A}{1+\frac{\alpha\rho}{m}\Pi}\left[P + b\frac{v}{s} + \frac{\alpha\rho}{m}E\right]$$

EXPERIMENTAL METHODS

16. Use was made of the NRL apparatus for getting data to determine instantaneous velocity values. With use of the apparatus a shadow-graph is obtained of the tail of a bullet, which, in effect, passes before an illuminated slit and casts a shadow on a photographic film, which rotates at a known speed behind the slit. The apparatus has been described in detail in references 2 and 3. A schematic drawing of the apparatus is shown in Plate 1. The major changes in the apparatus since the date of reference 3 have been the movement of the optical slit from near the trajectory to a position near the photographic film, with a separation of only about 0.003 in., and the changing of the collimating lenses by substituting a cylindrical lens of a larger aperture and an achromatic spherical lens. The resulting finer and brighter light beam gave a sharper trace. The method of measuring the film and the data analysis to determine the velocity of the nose of the bullet and the force resisting its penetration have been described in reference 3.

17. Plate 2 shows an enlargement of a shadow-graph of a partial penetration of a conical projectile. Shadow-graphs were made of impacts of conical ended Cal.30 projectiles on STS armor plate. The included angle of the conical ends was 45°. The steel projectiles were hardened

to about 65 Rockwell C, and each weighed about 120 grains. The STS specimens were of uniform hardness, 256 Brinell, measured 3 x 3 x 3/4 inches, and weighed about 1.8 pounds.

18. Since gun powder was used to propel the projectiles, a black residue of the exploded gun powder was deposited on the projectiles. Such a deposit made the degree of lubrication uncertain, but nevertheless effects of lubrication were observed. Three different conditions of lubrication were tried. In one the cones were bathed in benzene and allowed to dry before shooting. In another they were cleaned with benzene, dipped in a saturated solution of stearic acid in benzene, and allowed to stand until the benzene had evaporated. Also they were used as they came from the shop filmed with oil . Those cones which were washed and dried before shooting will be referred to as the "dry" cones, but the reader should bear in mind that the dry cones bore a coating of residue of exploded gun powder.

19. The steel projectiles bearing an oil film were shot with velocities ranging from 665 ft/sec to 2500 ft/sec. Those dry and those coated with stearic acid ranged in velocity from 300 ft/sec to 750 ft/sec. With higher velocities the projectiles penetrated beyond the bourrelet so that only that part of the penetration of a depth equal to the height of the cone was useful.

20. For comparisons with dynamic indentations, static indentations were made on a Brinell machine with a conical steel indenter of a 45° included angle, lubricated with stearic acid in one case and clean in the other. The clean case was achieved by previous washing in zylol. In each case indentations were made by applying the load in the usual manner. The depth of penetration was measured by use of a traveling microscope and

noting the position of the indenter at contact with the plate and its position at the end of the penetration.

RESULTS

21. In the course of trying various methods of analysis of the data collected for this report, discoveries were made of possibilities of greater precision in experimental techniques which would have improved the accuracy of the analyses. Most discrepancies occurring in the experimental results can be accounted for by these inaccuracies. Those data were chosen which best illustrate the experimental interpretations.

22. The data of the oil lubricated cones which ranged in velocity from 665 ft/sec to 3500 ft/sec were useful in showing up the terms involving the straining speed and α and for the evaluation of α. In Tables 1 through 6 are recorded the data and calculations of six of the impacts. The force values appearing in these tables are graphically smoothed values obtained by plotting the experimental determined force values against the squares of the corresponding depths. These graphs appear in Plate 3. The velocity and depth measurements recorded in the tables are those corrected for plate motion and bullet vibration.

23. Plate 4 is a graph showing plots of resistance values, $\frac{F}{A}$ against $\frac{v^2}{d}$ for the si impacts. Shown in Plate 5 are plots of $\frac{F}{A}$ against $E - \frac{4}{3}F$. From the $\frac{F}{A}$ versus $\frac{v^2}{d}$ graphs were chosen $\frac{F}{A}$ values at a $\frac{v^2}{d}$ value of 1.14×10^{-5} $(sec)^{-1}$, and from the $\frac{F}{A}$ versus $E - \frac{4}{3}F$ graph were found the corresponding $E - \frac{4}{3}F$ values. Plots of these values appear in Plate 6. The slope of the linear average gave an α value of 0.7.

24. Plate 7 shows plots for examination of $\frac{F}{A} - \frac{\alpha\rho}{m}\left(E - \frac{4}{3}F\right)$ as a function of $\frac{v}{a}$. Though the plots for the six impacts do not lie on the same curve they are no longer separated in the order of increasing velocities as they are in Plate 4. Part of their separation can be attributed to errors in depth measurements due to uncertain bluntness of the cones. Also there is a cumulative error in the operations to determine $\frac{F}{A}$. Though the exact function of the resistance with respect to $\frac{v}{a}$ may not be determined from this plot, it is clear that the resistance may be considered a function of $\frac{v}{a}$.

25. That a linear variation of $\frac{F}{A}$ with $\frac{v}{a}$ is a good approximation is demonstrated by plotting $\frac{E_0 - E}{\Omega} - \frac{\alpha\rho}{m}E$ against $\frac{k}{\Omega}\int v s\, ds$ (see paragraph 14) for three of the six impacts used in the study of $\frac{F}{A}$. This graph is shown in Plate 8. The impact velocities were 814 ft/sec, 1226 ft/sec, and 2521 ft/sec. Other pertinent data are given in Tables 7, 8 and 9. Data for the dry cones can also be represented by a linear approximation. Tables 10, 11, and 12 contain the data of three impacts with dry cones. Their impact velocities were 350 ft/sec, 525 ft/sec, and 768 ft/sec. Plate 9 shows a plot of $\frac{E_0 - E}{\Omega} - \frac{\alpha\rho}{m}E$ against $\frac{k}{\Omega}\int v s\, ds$ for the dry cones. Though not all of the plots follow the same curve, two nearly do, and all of the plots are approximately linear and have about the same slope. The line drawn has a slope of 1.6 lb sec/in^2. Using this value for k 0.7 for α, and 435×10^3 lb/in^2 for P, force values were calculated by use of equation (24) and substitution of the data of impact

#184, which had an initial velocity of 768 ft/sec. The results of the calculations are recorded in Table 13. In Table 14 are recorded the experimentally determined force values and the corresponding depths. In Plate 10 is shown a comparison of the experimentally determined force values and the calculated force values. The agreement is very close.

26. In Table 13 is also shown the contributions of the velocity and strain rate dependent forces to the total force resisting penetration. Their contributions are greatest near the beginning of the penetration, decreasing with depth. Near the middle of the penetration about 15% of the force resisting penetration is dependent upon strain rate, b term, and about 3% dependent upon velocity, α term.

27. The data is well represented by a linear variation of resistance with straining speeds in a range of 2.6×10^5 to 0.2×10^5 $(sec)^{-1}$. The higher straining speed is the greatest that occurred at a depth of 0.1 inch. At depths less than 0.1 inch uncertainties of geometry of the point greatly influence the calculations of resistance values. Below straining speeds of 0.2×10^5 $(sec)^{-1}$ the penetration resisting forces that are dependent on strain rates are so small as to be negligible.

28. In a comparison of the results of one impact with another, an important source of error is the lack of correction for bluntness. The bluntness of the cones was not noted before shooting them, and they were very likely blunted, for not a great deal of care was taken to perserve a very sharp point. In future studies of a similar nature to that of this report, care will be taken to note the amount of bluntness. Probable errors in force determinations have been discussed in the appendix of this report. Another variable influencing the results are differences

in lubrication.

29. Comparison of lubrication effects can best be made by comparing the total energy loss per unit volume for the various impacts. In Table 15 are recorded the calculations of total energy loss E_T, total volume of material displaced, Ω_T, and $\frac{E_T}{\Omega_T}$ for impacts of the "dry" condition, and for coatings of stearic acid, and of oil. Plate 11 shows plots of E_T against Ω_T. It is clear that lubrication does reduce resistance to penetration, but the stearic acid appears no better than the oil, there being considerable variation in the results. Bluntness can not account for all of this variation. Probably the same conditions of lubrication were not repeated each time, due to variations in effects of the exploded gun powder. Lubrication effects were also found in an examination of the indentation in the plate.

30. In the case of the impacts made with cones previously cleaned with benzene, there occurred much roughing of the surfaces of the cones and of the indents. The roughening extended from the vertex along the surface for a distance less than the slant height. We judged this roughening was caused by fusion of the plate and cone materials. In the case of the stearic acid coated cones fusion occurred only very near the tip of the cone. In Table 16 are recorded some measurements to show the difference in extent of fusion in the cases of the stearic acid coated and dry cones. The diameter at the base of the roughened surfaces of the indentations were measured. On an average the area of fusion in the dry case was twelve times as great as that of the stearic acid case.

31. The static penetrations were greatly influenced by lubrication. The depth of penetration was increased from 0.1293 inches for a cone previously cleaned with zylol to 0.1687 inches for a stearic acid coated cone. This represented a change in hardness number from 734×10^3 to 431×10^3 lb/in^2. In the clean case the indenter point stuck in the plate, and was found broken near the level of the plate surface on release of the load. In several repeated trials of the clean case the points stuck in the plate and broke off. In the lubricated case it was found that only the very tip of a finely pointed cone stuck in the plate. Bluntness of the indenter affects the depth of penetration to a marked degree. A stearic acid coated cone, whose height lacked 0.006 inches of being the height calculated from measurement of its diameter at its base, penetrated to a depth of only 0.1542 inches. Correction for bluntness by addition 0.006 inches to the depth of penetration gave 0.1619 inches for the height of the conical indentation, about 0.007 inches short of the height of the indentation made with a very sharp cone.

CONCLUSIONS

32. The resistance to penetration of a cone into a solid medium can be expressed as a function of straining speed and the kinetic energy of plate material set in motion about the penetrating cone. For the range of straining speeds, 0.2×10^5 (sec)$^{-1}$ to 2.6×10^5 (sec)$^{-1}$ occurring in these experiments, the results may be approximately represented in equation form as:

$$\frac{F}{A} = -\frac{dE}{d\Omega} = \frac{1}{1 + \frac{\alpha\rho}{m}\Omega}\left[P + b\frac{v}{s} + \frac{\alpha\rho}{m}E\right]$$

For studies of small energy losses in the dynamics of armor penetration lubrication effects are important.

33. A more careful analysis could have been made had attention been paid to bluntness conditions prior to shooting the projectiles.

34. Using the improved procedures indicated by this preliminary work future studies can give determinations of α, b and P which are more precise and cover a wider range of velocities and straining speeds.

[redacted]

REFERENCES

1. NRL Report No. O-2376; "Some Dynamic Hardness Tests on Plastics"; 25 September 1944.
2. NRL Report No. O-1591 "Sixth Partial Report on Light Armor. The Dynamics of Armor Penetration by Small Projectiles"; 6 Feb. 1940.
3. NRL Report No. O-2276; "The Measurement of Forces Which Resist Penetration of STS Armor, Mild Steel, and 24 ST Aluminum"; April 1944.

[redacted]

APPENDIX

Probable Errors in Force Determinations

In view of the improvements made in the apparatus and methods for obtaining force data on the penetration of armor by projectiles it has become desirable to reconsider the errors which occur and their effect on the computed force. This will bring up to date the investigation made in connection with reference 2, a description of which is contained in Appendix B of that report.

The errors will be discussed individually as to extent. Any probable error of one-quarter of one percent (0.25% or 0.0025) is considered to be insignificant. The sources of error are:

(1) Measurement of the turbine velocity

(2) Measurement of film length

(3) Measurement of the Reduction Factor

(4) Measurement of the projectile length

(5) Measurement of the projectile mass

(6) Projectile yaw

(7) Determination of the position of impact

(8) Alignment of film in comparator

(9) Crosshair settings for displacements

(10) Accuracy of comparator

(11) Determination of bullet period

(12) Slope measurement

(13) Film distortion

The probable error (P.E.) was determined in each case from a series of no less than twenty-five actual measurements. In some cases these were repeated by a second observer. The P. E. was computed by the formula:

$$P.E. = 0.6745 \sqrt{\frac{x_1^2 + x_2^2 + \cdots + x_n^2}{n}}$$

where $x_1, x_2 \cdots x_n$ are the deviations of the actual measurements from the arithmetical mean of these measurements and n, the number of measurements. Combinations of probable errors were determined by the following formulas:

Sum and difference: P.E. of $(a \pm \Delta a) \pm (b \pm \Delta b) =$

Δa or Δb, whichever is larger

Product: $$P.E._{(ab)} = ab \sqrt{\left(\frac{P.E._{(a)}}{a}\right)^2 + \left(\frac{P.E._{(b)}}{b}\right)^2}$$

Quotient: $$P.E._{\left(\frac{a}{b}\right)} = \frac{a}{b} \sqrt{\left(\frac{P.E._{(a)}}{a}\right)^2 + \left(\frac{P.E._{(b)}}{b}\right)^2}$$

In computing the projectile velocity from the data obtained by reading the film, the velocity, and consequently the force, is proportional to the linear velocity of the drum. The rotational velocity of the turbine is indicated on a scale which can be read accurately to $\pm$ 0.2 cycle/sec. At speeds of 450 rps this would be a maximum error of $\pm$ 0.04 %. In reading the scale of the oscillator there is a correction to be made as set forth in the calibration data chart supplied with

the instrument. This is interpolated over the range of frequencies used and is figured only to the nearest tenth of a cycle per second. This results in an additional possible error of ± 0.05 rps which at speeds of 450 rps would be a maximum error of $\pm 0.01\%$. In the case of the rotational velocity of the turbine it is impossible to duplicate conditions with sufficient accuracy to take the number of repeated readings necessary for determining the P.E. by the usual method. So it was decided arbitrarily to take the maximum errors, which here are very small, as the P. E. The final P.E. will be ± 0.2 rps or $\pm 0.04\%$ at an average speed, which is negligible. The linear velocity of the drum is also proportional to the film length. Two series of measurements of the internal diameter of the drum were made, one with a vernier caliper and the other with an internal micrometer. In both cases the P.E. was $\pm 0.013\%$ which is negligible.

Measurement of the reduction factor (R.F.), the ratio between the image on the film and the object, introduces a P.E. of $\pm 0.1\%$ which is negligible.

A measurement of the length of the projectile is used only to determine the point of impact on the film and does not enter into calculation of the forces. A series of measurements was taken and the P.E. of an average projectile of the type used was computed to be ± 0.00004 inch or $\pm 0.001\%$. Since this is so small it may be neglected.

The projectile mass is used in computing the forces. The P.E. in the measurement of this quantity was found to be ± 0.0045 grain or $\pm 0.004\%$. This is considered negligible in its effect on the force.

Yaw gives rise to errors in the position at impact and in the force. A desirable condition for the present series of shots was normal impact. However, since this is difficult to obtain under the experimental conditions, it was decided to include in the study those having slight yaw. All with more than 3° yaw were rejected and most of those retained had much less. In computing the P.E. due to yaw it will be based on the maximum of 3°.

The effect of yaw on forces is not completely understood. In general, the direct effect is an increase in the forces but it is not known through which quantity used in computing the forces this effect acts. If the Constant Pressure Theory is applied as a first approximation, it is seen that in order to keep the pressure constant as the projected area increases with the tilting of the bullet, the forces must increase in proportion to increase in area. For the cone portion the increase in area may be computed by a more complicated process to be 0.3% resulting in an error in forces of that amount. For the cylindrical portion of the projectile, however, it is easily seen that the increase in area is proportional to the secant of the angle of yaw. This is the difference between the area of a circular cross-section and an elliptical area having one semi-axis equal to the radius of the circle and the other axis greater by a factor equal to the secant of the angle. The measured forces resisting penetration by a yawed projectile are, therefore, larger by a factor equal to the secant of the angle of yaw than the forces resisting a normal projectile under the same conditions. If the bullet is yawed by as much as 3°, the maximum imposed, the corresponding forces of a normal projectile would be less than those computed by only 0.14%. This amount lies well within the limit of experimental

in the alignment so easily detected that it is believed to be practically impossible to effect an appreciable change in the forces because of misalignment. Likewise, it can be shown geometrically that errors in displacement, position of impact and time due to a slight rotation are insignificant and can be neglected.

In addition to the possible error in displacement due to rotation of the film, there may be an error incurred in placing the crosshair on the trace. A minimum error is completely dependent upon the ability of the reader to place the cross hair consistently at the same relative position in the fringe at the edge of the trace. The positions are read to four decimal places on a centimeter scale. From experience an observer can say that repeated readings never vary by as much as 0.001 cm, or about 0.0004 inch. For the average total displacement this is a negligible error, but for the individual reading it may represent an error of as high as 7% in the lower velocity ranges. However, the error cannot be cumulative but is subject to statistical fluctuations. If the velocities are computed from the displacements they will show the same fluctuations but the trend can be determined by a smoothing process. This error has no effect on the forces when the velocities are computed from slope measurements.

The accuracy of the comparator used for making the measurements was checked by a series of measurements of the distance between two parallel lines one mil apart, made over the range of the vertical and horizontal scales used. The average deviation from the mean for the horizontal motion was 0.0002 mm and for the vertical 0.0003 mm. The error is negligible as far as displacements are concerned since they are not read to this place, and has no effect upon the velocities and

forces.

The period of vibration of the projectile during penetration is perhaps the most uncertain quantity dealt with in this method of determining the forces resisting penetration. Because of this and the fact that its use in computing the forces cannot be directly expressed mathematically it is difficult to determine accurately the extent of error due to this quantity. From one film showing clearly the vibrations of the projectile as it rebounded the period of the bullet in flight was measured to be nine microseconds. The period during penetration is a difficult thing to measure since the vibrations are a modulation of a changing function which is influenced by unknown errors. In actual calculations from data on force-time curves an average of the time between successive dips was the same as that for a projectile in free flight. A probable error determined from the deviations from this mean was $\pm 16.8\%$. Although the bullet period appears in the denominator of the expression used in computing forces an error of this size does not result in a similar error in the force. The numerator contains a factor which is the difference of two instantaneous velocities, the time between them being determined by the period of the projectile. Thus the error enters into this quantity in some indirect way which cannot be definitely expressed and the resultant error in the force is not known. In order to tell more definitely the effect of an error in the period on the forces over a complete penetration the root mean square error was considered. The forces were computed from one set of data with nine microseconds as the bullet period. The same data were used to compute forces on the basis of seven and eleven microsecond periods which would be equivalent to 22% error in the period. Using the devia-

tions from the forces based on a nine microsecond period taken at regular intervals along the curve the root mean square error was found to be $\pm$ 2.04% for a period of seven microseconds and $\pm$ 1.64% for a period of eleven microseconds. The forces for periods of eight, and nine and eight-tenths, microseconds were also computed but not the root mean square errors. However, when these are plotted with the other three force curves as shown in Plate 12 it is seen that they do not as a whole deviate from the mean as much as the seven microsecond curve. It is believed, then, for no period within the computed P.E. will the error in the force amount to more than 2%.

In studying the error of the slope measurements the character of the film must be taken into consideration. Films varying in density, contrast, sharpness of trace and amount of curvature were selected for the investigation. Readings were made by two observers at several points on each film and at different relative positions in the band in which the density changes from a maximum to a minimum. At no point was there an error of more than 1%. Curvature was computed for some points but there seemed to be no relation between that and error in slope reading. It is concluded that the most predominant influence on the error is the character of the photograph itself, although the placing of the crosshair seems to have some effect.

The total error affecting the forces as a result of all individual measurable errors, including those described as negligible but excluding those due to yaw and error in bullet period, was computed to be 1.006%. The total of this and the errors which do not enter directly into the formula for computing forces, namely those due to yaw and bullet period

measurement, was taken as the square root of the squares of the quantities and was evaluated to be 2.26%. There may be additional errors due to judgment, fatigue and those inherent in the system itself. An effort was made to investigate the last of these. The foregoing treatment of slope error pertained only to a measure of the accuracy with which readings can be repeated and does not attempt to show the precision with which actual slope values may be measured. The latter was investigated by comparing the old and accurate method of computing forces directly from displacements and the new method of computing forces from slopes.

The first step consisted in measuring angles, of which the magnitude could also be computed from known measurements, to see how accurately one can estimate the slope at points along a curve. The image of a circle was used for this. The measured angles agreed with the computed values to within ten minutes. This is the equivalent of three of the smallest divisions on the scale read and does not represent a serious error for unsmoothed primary data. The slope method was then checked against the displacement method by integrating the slope values and comparing them with the displacements. This was done both for the circle readings and some actual shots. Most of the results showed a cumulative effect of the error in the slope. No explanation could be found for this other than that the errors must not have a normal distribution. The error generally totalled a few thousandths of a centimeter and is not considered serious. The fact that in some cases the error tended to become constant after the slope had decreased to 45°, and the fact that there seems to be a velocity effect, with the errors for high velocity shots being greater, lead us to believe that the error could be partially eliminated if the slopes are kept low enough. This

could be done through increased drum speed.

There existed the possibility that the present optical system caused distortion of the image produced on the film. It was determined from a series of measurements comparing the size of intervals on a finely graduated scale and on a shadowgraph of the scale that this distortion is negligible.

The preceding discussion of errors applies only to determination of force. When the results are used in a theoretical framework such as that illustrated in this report, estimates of the precision of the quantities derived indirectly from the force data require additional considerations which are not treated in detail in this appendix. For example, due to small angles of yaw at impact resisting forces will begin before the time predicted by the length of the projectile. Also, due to lack of sharpness of the cone point, an error occurs in the calculation of values of force per unit area. In both cases the errors reduce rapidly as the embedded volume of the penetrator increases. These errors are important in furnishing an upper limit on the high straining speeds for which the results can be used with confidence.

[redacted]

TABLE 1

Impact #115 V_s = 7979 in/sec. (Striking Velocity)

$E = 2.242 \times 10^{-5} v^2$ $\rho = 0.283$ lb/in^3 m = 121.12 gr. $\frac{\rho}{m} = 16.4 \left(\frac{1}{in^3}\right)$

$\frac{v}{s} \times 10^{-5}$ (sec^{-1})	F (lb)	A $\times 10^{2}$ (in^2)	$\frac{F}{A} \times 10^{-3}$ (lb/in^2)	E $\times 10^{-3}$ (in lb)	$\frac{sF}{3} \times 10^{-3}$ (in lb)	$(E - \frac{sF}{3}) \times 10^{-3}$ (in lb)	$\frac{\rho}{m}(E - \frac{sF}{3}) \times 10^{-3}$ (lb/in^2)	$\frac{F}{A} - \frac{\rho}{m}(E - \frac{sF}{3}) \times 10^{-3}$ (lb/in^2)
1.59	700	.135	519	1.415	.012	1.403	15.99	503.01
1.30	1000	.201	498	1.406	.020	1.386	15.80	482.20
1.08	1470	.287	512	1.390	.036	1.354	15.44	496.56
1.01	1670	.328	509	1.381	.043	1.338	15.25	493.75
.865	2150	.437	492	1.359	.066	1.293	14.74	477.26
.763	2650	.550	482	1.332	.091	1.241	14.15	467.85
.609	3700	.814	455	1.260	.156	1.104	12.59	442.41
.520	4610	1.056	437	1.186	.221	.965	11.00	426.00
.430	5910	1.396	423	1.072	.322	.750	8.55	414.45
.356	7300	1.768	413	.930	.442	.488	5.56	407.44
.298	8650	2.134	405	.787	.570	.217	2.47	402.53
.233	10,390	2.609	398	.592	.752	-.160	-1.82	399.82
.167	12,280	3.132	392	.361	.982	-.621	-7.08	399.08
.128	13,200	3.396	389	.231	1.117	-.886	-10.10	399.10
.087	14,080	3.644	386	.114	1.257	-1.143	-13.03	399.03
.058	14,380	3.730	386	.052	1.312	-1.260	-14.36	400.36

[redacted]

(1)

TABLE 2

Impact #108 V_s = 9767 in/sec.

$E = 2.239 \times 10^{-5} v^2$ $\rho = 0.283$ lb/in^3 m = 120.94 gr. $\frac{\rho}{m} = 16.4 \left(\frac{1}{in^3}\right)$

$\frac{v}{s} \times 10^{-5}$ (sec^{-1})	F (lb)	A x 10^2 (in^2)	$\frac{F}{A} \times 10^{-3}$ (lb/in^2)	E x 10^{-3} (in lb)	$\frac{sF}{3} \times 10^{-3}$ (in lb)	$(E - \frac{sF}{3}) \times 10^{-3}$ (in lb)	$\frac{\alpha\rho}{m}(E - \frac{sF}{3}) \times 10^{-3}$ (lb/in^2)	$\frac{F}{A} - \frac{\alpha\rho}{m}(E - \frac{sF}{3}) \times 10^{-3}$ (lb/in^2)
1.91	900	.140	643	2.118	.015	2.103	24.18	618.82
1.49	1320	.228	579	2.100	.029	2.071	23.82	555.18
1.20	1870	.345	542	2.078	.050	2.028	23.32	518.68
1.02	2470	.476	519	2.049	.077	1.972	22.68	496.32
.88	3150	.629	501	2.011	.113	1.898	21.83	479.17
.77	3960	.802	494	1.964	.161	1.803	20.73	473.27
.68	4800	.997	481	1.903	.218	1.685	19.38	461.62
.60	5700	1.213	470	1.832	.285	1.547	17.79	452.21
.54	6720	1.450	463	1.751	.367	1.384	15.92	447.08
.49	7660	1.689	453	1.655	.452	1.203	13.83	439.17
.44	8700	1.946	446	1.549	.551	.998	11.48	434.52
.40	9710	2.199	441	1.437	.654	.783	9.00	432.00
.36	10760	2.468	439	1.317	.768	.549	6.31	432.69
.32	11750	2.729	430	1.187	.881	.306	3.52	426.48
.29	12820	3.002	427	1.057	1.009	.048	.55	426.45
.26	13800	3.262	423	.927	1.132	- .205	- 2.36	425.36
.23	14720	3.505	419	.799	1.251	- .452	- 5.20	424.20
.21	15660	3.757	416	.667	1.378	- .711	- 8.18	424.18
.18	16500	3.988	417	.540	1.496	- .956	-10.99	427.99
.16	17270	4.196	411	.423	1.606	-1.183	-13.60	424.60
.13	18020	4.409	409	.318	1.718	-1.400	-16.10	425.10
.11	18480	4.533	408	.222	1.786	-1.564	-17.99	425.99
.08	18950	4.659	407	.137	1.857	-1.720	-19.78	426.78

(2)

TABLE 3

Impact #270 V_s = 14,706 in/sec.

$E = 2.267 \times 10^{-5} v^2$ $\rho = .283$ lb/in^3 m = 122.5 gr. $\frac{\rho}{m} = 16.2 \left(\frac{1}{in^3}\right)$

$\frac{v}{s} \times 10^{-5}$ (sec^{-1})	F (lb)	A $\times 10^2$ (in^2)	$\frac{F}{A} \times 10^{-3}$ (lb/in^2)	E $\times 10^{-3}$ (in lb)	$\frac{sF}{3} \times 10^{-3}$ (in lb)	$(E - \frac{sF}{3}) \times 10^{-3}$ (in lb)	$\frac{\alpha\rho}{m}(E - \frac{sF}{3}) \times 10^{-3}$ (lb/in^2)	$\frac{F}{A} - \frac{\alpha\rho}{m}(E - \frac{sF}{3}) \times 10^{-3}$ (lb/in^2)
1.45	3,000	.539	557	4.787	.100	4.687	52.96	504.04
1.18	4,440	.803	553	4.707	.181	4.526	51.14	501.86
.99	5,940	1.100	539	4.590	.283	4.307	48.67	490.33
.85	7,700	1.466	525	4.446	.424	4.022	45.45	479.55
.74	9,520	1.865	510	4.269	.590	3.679	41.57	468.43
.65	11,420	2.307	494	4.055	.788	3.267	36.92	457.08
.57	13,530	2.776	487	3.808	1.024	2.784	31.46	455.54
.51	15,520	3.261	476	3.526	1.273	2.253	25.46	450.54
.45	17,620	3.784	466	3.223	1.556	1.667	18.84	447.16
.40	19.730	4.317	457	2.899	1.861	1.038	11.73	445.27
.35	21,650	4.851	446	2.557	2.165	.392	4.43	441.57

TABLE 4

Impact #271 V_s = 18,333 in/sec.

$E = 2.264 \times 10^{-5} v^2$ $\rho = 0.283$ lb/in^3 m = 122.33 gr. $\frac{\rho}{m} = 16.4 \left(\frac{1}{in^3}\right)$

)	$\frac{v}{s} \times 10^{-5}$ (sec^{-1})	F (lb)	A x 10^2 (in^2)	$\frac{F}{A} \times 10^{-3}$ (lb/in^2)	E x 10^{-3} (in lb)	$\frac{sF}{3} \times 10^{-3}$ (in lb)	$(E - \frac{sF}{3}) \times 10^{-3}$ (in lb)	$\frac{\alpha\rho}{m}(E - \frac{sF}{3}) \times 10^{-3}$ (lb/in^2)	$\frac{F}{A} - \frac{\alpha\rho}{m}(E - \frac{sF}{3}) \times 10^{-3}$ (lb/in^2)
	1.85	3,200	.518	618	7.480	.105	7.375	83.34	534.66
	1.44	5,170	.843	614	7.363	.215	7.148	80.77	533.23
	1.29	6,300	1.041	606	7.283	.292	6.991	79.00	527.00
	1.06	8,730	1.485	588	7.087	.483	6.604	74.63	513.37
	.98	10,030	1.727	581	6.965	.598	6.367	71.95	509.05
	.83	13,050	2.288	570	6.666	.896	5.770	65.20	504.80
	.77	14,620	2.585	566	6.492	1.067	5.425	61.30	504.70
	.67	17,750	3.209	553	6.086	1.444	4.642	52.45	500.55
	.59	20,980	3.900	538	5.613	1.881	3.732	42.17	495.83
	.51	23,780	4.596	517	5.101	2.315	2.786	31.48	485.52
	.45	26,130	5.348	489	4.563	2.744	1.819	20.55	468.45

[redacted]

TABLE 5

Impact #277 V_s = 25,758 in/sec.

$E = 2.256 \times 10^{-5} v^2$ $\rho = 0.283$ lb/in^3 m = 121.88 gr. $\frac{\rho}{m} = 16.3 \left(\frac{1}{in^3}\right)$

)	$\frac{v}{s} \times 10^{-5}$ (sec^{-1})	F (lb)	A x 10^2 (in^2)	$\frac{F}{A} \times 10^{-3}$ (lb/in^2)	E x 10^{-3} (in lb)	$\frac{sF}{3} \times 10^{-3}$ (in lb)	$(E - \frac{sF}{3}) \times 10^{-3}$ (in lb)	$\frac{\alpha\rho}{m}(E - \frac{sF}{3}) \times 10^{-3}$ (lb/in^2)	$\frac{F}{A} - \frac{\alpha\rho}{m}(E - \frac{sF}{3}) \times 10^{-3}$ (lb/in^2)
	2.207	5,000	.725	690	14.78	.193	14.59	166.33	523.67
	1.882	6,730	.990	680	14.67	.304	14.37	163.82	516.18
	1.639	8,600	1.291	666	14.52	.444	14.08	160.51	505.49
	1.448	10,700	1.632	656	14.32	.621	13.70	156.18	499.82
	1.295	13,020	2.008	648	14.09	.838	13.25	151.05	496.95
	1.169	15,470	2.418	640	13.82	1.092	12.73	145.12	494.88
	1.064	18,100	2.859	633	13.54	1.389	12.15	138.51	494.49
	.8916	23,630	3.840	615	12.78	2.102	10.68	121.75	493.25
	.8213	26,300	4.369	602	12.34	2.496	9.84	112.18	489.82
	.7585	28,770	4.926	584	11.86	2.899	8.96	102.14	481.86
	.7024	30,600	5.499	556	11.36	3.258	8.10	92.34	463.66

[redacted]

TABLE 6

Impact #275 V_s = 30,246 in/sec.

$E = 2.262 \times 10^{-5} v^2$ $\rho = 0.283$ lb/in^3 m = 122.23 gr. $\frac{\rho}{m} = 16.2(\frac{1}{in^3})$

c)	$\frac{V}{s} \times 10^{-5}$ (sec^{-1})	F (lb)	A x 10^2 (in^2)	$\frac{F}{A} \times 10^{-3}$ (lb/in^2)	E x 10^{-3} (in lb)	$\frac{sF}{3} \times 10^{-3}$ (in lb)	$(E - \frac{sF}{3}) \times 10^{-3}$ (in lb)	$\frac{\alpha\rho}{m}(E - \frac{sF}{3}) \times 10^{-3}$ (lb/in^2)	$\frac{F}{A} - \frac{\alpha\rho}{m}(E - \frac{sF}{3}) \times 10^{-3}$ (lb/in^2)
	2.59	5,800	.725	800	20.38	.224	20.16	227.81	572.19
	2.15	8,050	1.043	772	20.21	.373	19.84	224.19	547.81
	1.83	10,830	1.418	764	19.99	.586	19.40	219.22	544.78
	1.60	13,750	1.845	745	19.71	.848	18.86	213.12	531.88
	1.41	16,950	2.332	727	19.36	1.175	18.18	205.43	521.57
	1.26	20,280	2.851	711	18.96	1.555	17.40	196.62	514.38
	1.13	23,650	3.426	690	18.49	1.987	16.50	186.45	503.55
	1.03	27,050	4.047	668	17.96	2.471	15.49	175.04	492.96
	.94	30,200	4.716	640	17.36	2.978	14.38	162.49	477.51
	.86	33,000	5.416	609	16.72	3.487	13.23	149.50	459.50

[redacted]

TABLE 7

Impact #108 V_s = 9767 in/sec.

$E_o = 2.136 \times 10^3$ in lb. $\frac{\alpha\rho}{m} = 11.5 \left(\frac{1}{in^3}\right)$ k = 0.539

v (in/sec)	E x 10^{-3} (in lb)	E_o - E x 10^{-3} (in lb)	$\frac{E_o - E}{\pi} \times 10^{-3}$ (lb/in^2)	$\frac{\alpha\rho}{m}$ E x 10^{-3} (lb/in^2)	$\frac{E_o - E}{\pi} - \frac{\alpha\rho}{m}$ E x 10^{-3} (lb/in^2)	vs (in^2/sec)	$k\int vsds$ (in^3/sec)	$\frac{k\int vsds}{\pi} \times 10^{-6}$ (sec^{-1})
9725	2.118	.018	756	24.4	712	496	6.79	.285
9686	2.100	.036	730	24.2	706	630	11.05	.224
9633	2.078	.058	630	23.9	606	771	16.7	.182
9567	2.049	.087	583	23.6	559	899	23.0	.154
9475	2.011	.125	552	23.1	529	1023	30.3	.134
9363	1.964	.172	527	22.6	504	1142	38.5	.118
9221	1.903	.233	516	21.9	494	1254	47.5	.105
9046	1.832	.304	501	21.1	480	1357	57.3	.0945
8841	1.751	.385	486	20.1	466	1450	68.0	.0858
8597	1.655	.481	483	19.0	464	1522	78.4	.0787
8320	1.549	.587	476	17.8	458	1581	89.3	.0725
8011	1.437	.699	472	16.5	455	1618	99.7	.0673
7670	1.317	.819	465	15.1	450	1641	110.2	.0628
7282	1.187	.949	464	13.7	450	1638	119.9	.0586
6872	1.057	1.079	457	12.2	435	1622	129.6	.0549
6436	.927	1.209	452	10.7	441	1583	138.0	.0516
5971	.799	1.337	449	9.2	440	1523	145.5	.0488
5461	.667	1.469	444	7.7	436	1442	152.7	.0462
4910	.540	1.596	441	6.2	435	1336	158.7	.0439
4348	.423	1.713	439	4.8	434	1213	163.5	.0419
3767	.318	1.818	433	3.7	429	1077	167.8	.0399
3150	.222	1.914	437	2.6	434	914	170.1	.0388
2476	.137	1.999	438	1.6	436	728	171.7	.0376

TABLE 8

Impact #270 V_s = 14.706 in/sec.

$E_o = 4.903 \times 10^3$ in lb. $\frac{\alpha\rho}{m} = 11.3 \left(\frac{1}{in^3}\right)$ k = 0.539 $\Omega = .17967\ s^3\ (in^3)$

v (in/sec)	E x 10^{-3} (in lb)	E_o - Ex10^{-3} (in lb)	$\frac{E_o - E}{\Omega}$ x 10^{-3} (lb/in^2)	$\frac{\alpha\rho}{m}$ E x 10^{-3} (lb/in^2)	$\frac{E_o - E}{\Omega} - \frac{\alpha\rho}{m}$ E x 10^{-3} (lb/in^2)	vs (in^2/sec)	$k\int vsds$ (in^3/sec)	$\frac{k\int vsds}{\Omega}$ x 10^{-6} (sec^{-1})
14,531	4.787	.116	645.5	54.1	591	1453	39.2	.218
14,409	4.707	.196	600.7	53.2	548	1758	58.3	.179
14,230	4.590	.313	595.7	51.9	544	2035	79.7	.152
14,005	4.446	.457	566.2	50.2	516	2311	105.5	.131
13,723	4.269	.634	548.3	48.2	500	2552	133.0	.115
13,375	4.055	.848	532.1	45.8	486	2769	163.1	.102
12,960	3.808	1.095	521.0	43.0	478	2942	193.9	.092
12,472	3.526	1.377	514.8	39.8	475	3068	224.7	.084
11,923	3.223	1.680	502.5	36.4	466	3160	256.6	.077
11,308	2.899	2.004	492.1	32.8	459	3200	287.4	.071
10,621	2.557	2.346	483.6	28.9	455	3186	316.7	.065

[redacted]

TABLE I3

Impact #184 v_s = 9217 in/sec

39 s^2 Ω = 0.17967 s^3 α = 0.7 $\frac{\alpha\rho}{m}$ = 11.7 b = 1.6 P = 435 x 10^3 lb/in^2

	Ω x 10^5 (in^3)	$1 + \frac{\alpha\rho}{m}\Omega$	$\frac{A}{1 + \frac{\alpha\rho}{m}\Omega}$	$\frac{A\ b\ v/s}{1 + \alpha\rho m/\Omega}$ (lb)	$\frac{A\ \alpha\rho E/m}{1 + \alpha\rho m/\Omega}$ (lb)	$\frac{AP}{1 + \alpha\rho m/\Omega}$ (lb)	F (lb)	% F b term	% F α term
7	12.1	1.0014	.00416	686	87	1810	2583	27	3.4
3	30.1	1.0035	.00760	897	149	3306	4352	21	3.4
2	52.5	1.0061	.01095	1029	198	4763	5990	17	3.3
5	82.3	1.0096	.01471	1133	238	6399	7770	15	3.1
5	119.2	1.0139	.01879	1183	263	8174	9620	12	2.7
2	161.8	1.0189	.0229	1191	236	9962	11389	10	2.1
3	207.5	1.0243	.0269	1130	245	11702	13077	9	1.9
2	276.5	1.0324	.0324	972	175	14094	15241	6	1.1
0	349.4	1.0409	.0375	563	135	16313	17011	3	.8

[redacted]

TABLE 14

Impact #184

s (in)	F (lb)	s (in)	F (lb)
.0429		.1932	9919
.0493	899	.1983	10370
.0557	1070	.2032	10890
.0621	1310	.2080	11200
.0685	1660	.2127	11580
.0748	2040	.2173	11990
.0812	2320	.2218	12440
.0875	2660	.2261	12820
.0938	3040	.2302	13270
.1001	3390	.2342	13720
.1063	3800	.2381	14100
.1125	4150	.2418	14650
.1186	4458	.2452	14900
.1248	4838	.2485	15480
.1308	5322	.2517	15620
.1369	5737	.2546	15930
.1429	6324	.2575	16450
.1488	6739	.2602	16830
.1546	7188	.2626	17070
.1604	7741	.2648	17280
.1661	8156	.2669	17450
.1717	8502	.2688	17800
.1772	8813	.2705	17970
.1827	9193	.2719	18140
.1880	9573		

[redacted]

TABLE 15

DRY			OIL				STEARIC ACID			
10^{-3} lb)	$\Omega_T \times 10^{-5}$ $(in)^3$	$\frac{E_o}{\Omega_T} \times 10^{-3}$ (lb/in^2)	Impact No.	$E_o \times 10^{-3}$ (in lb)	$\Omega_T \times 10^{-5}$ $(in)^3$	$\frac{E_o}{\Omega_T} \times 10^{-3}$ (lb/in^2)	Impact No.	$E_o \times 10^{-3}$ (in lb)	$\Omega_T \times 10^{-5}$ $(in)^3$	$\frac{E_o}{\Omega_T} \times 10^{-3}$ (lb/in^2)
45	77.81	494	115	1.427	342.0	417	221	.3621	69.53	521
93	193.9	500	109	1.681	377.8	445	227	.9795	196.6	498
3	386.0	483	108	2.136	504.8	423	216	1.508	353.6	426
			152	1.096	212.9	515	219	.7631	171.2	445
							218	1.839	420.3	438

[redacted]

SCHEMATIC DIAGRAM OF APPARATUS

PLATE I

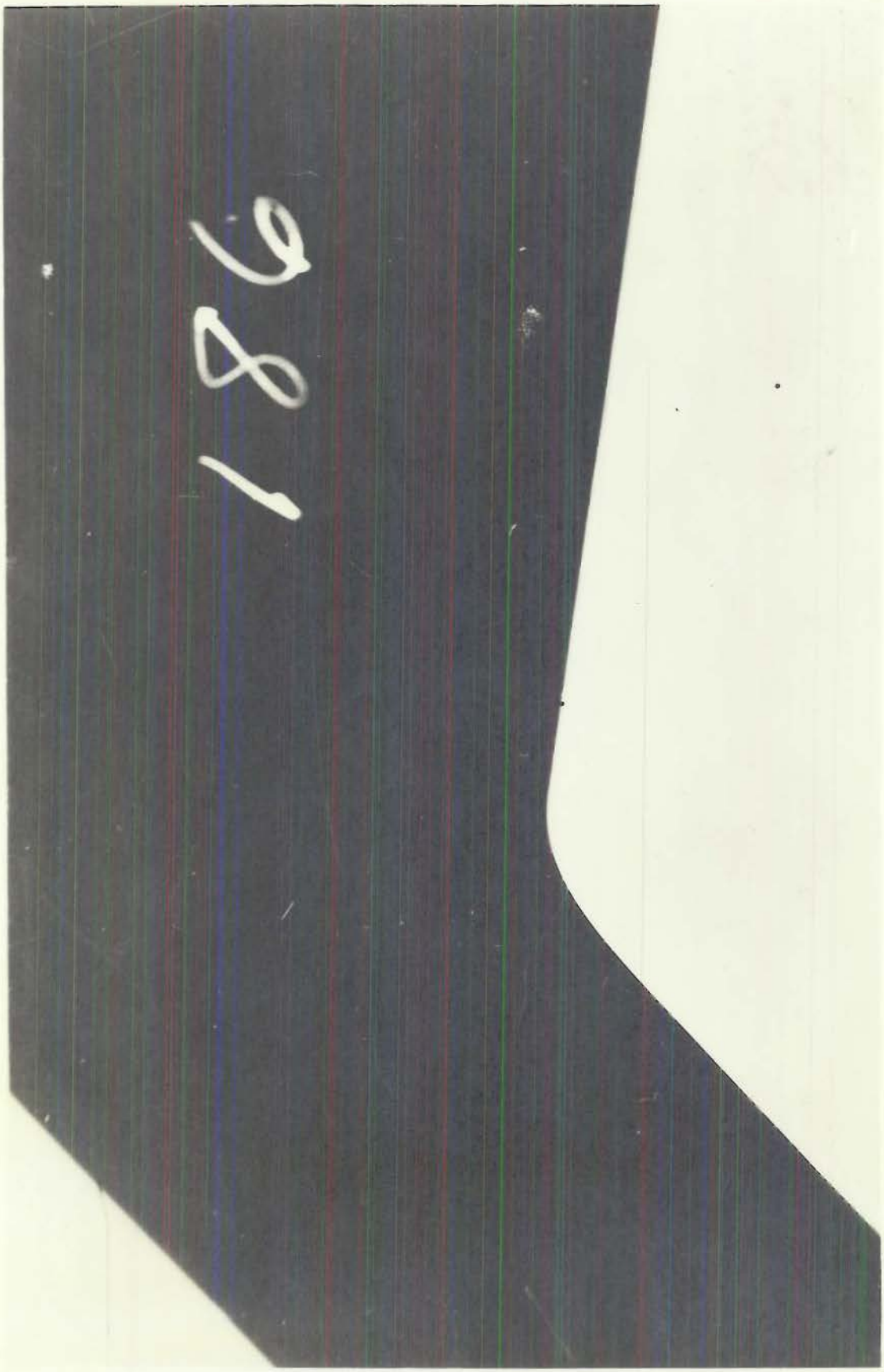

PLATE 2

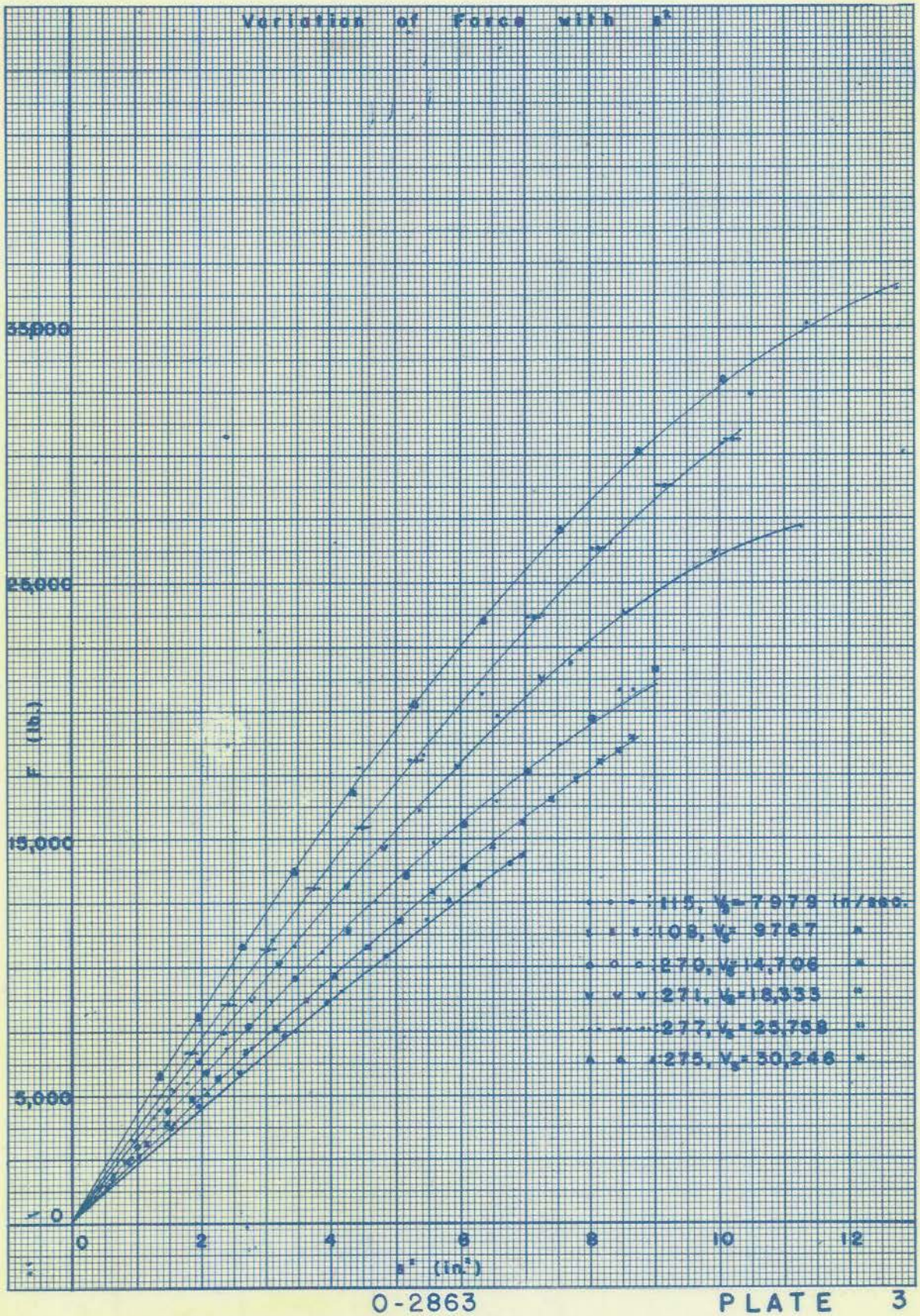

0-2863 PLATE 3

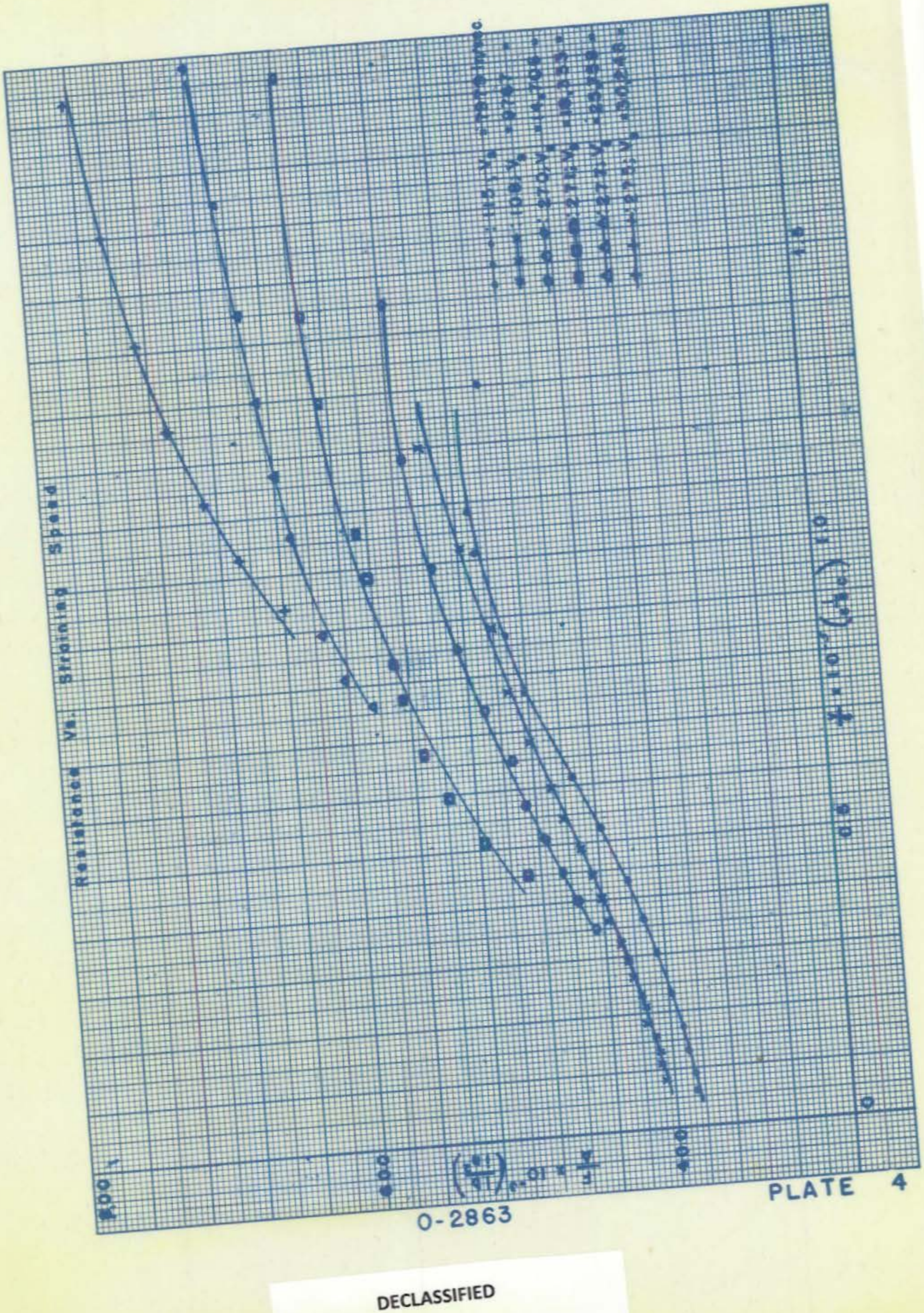

0-2863

PLATE 4

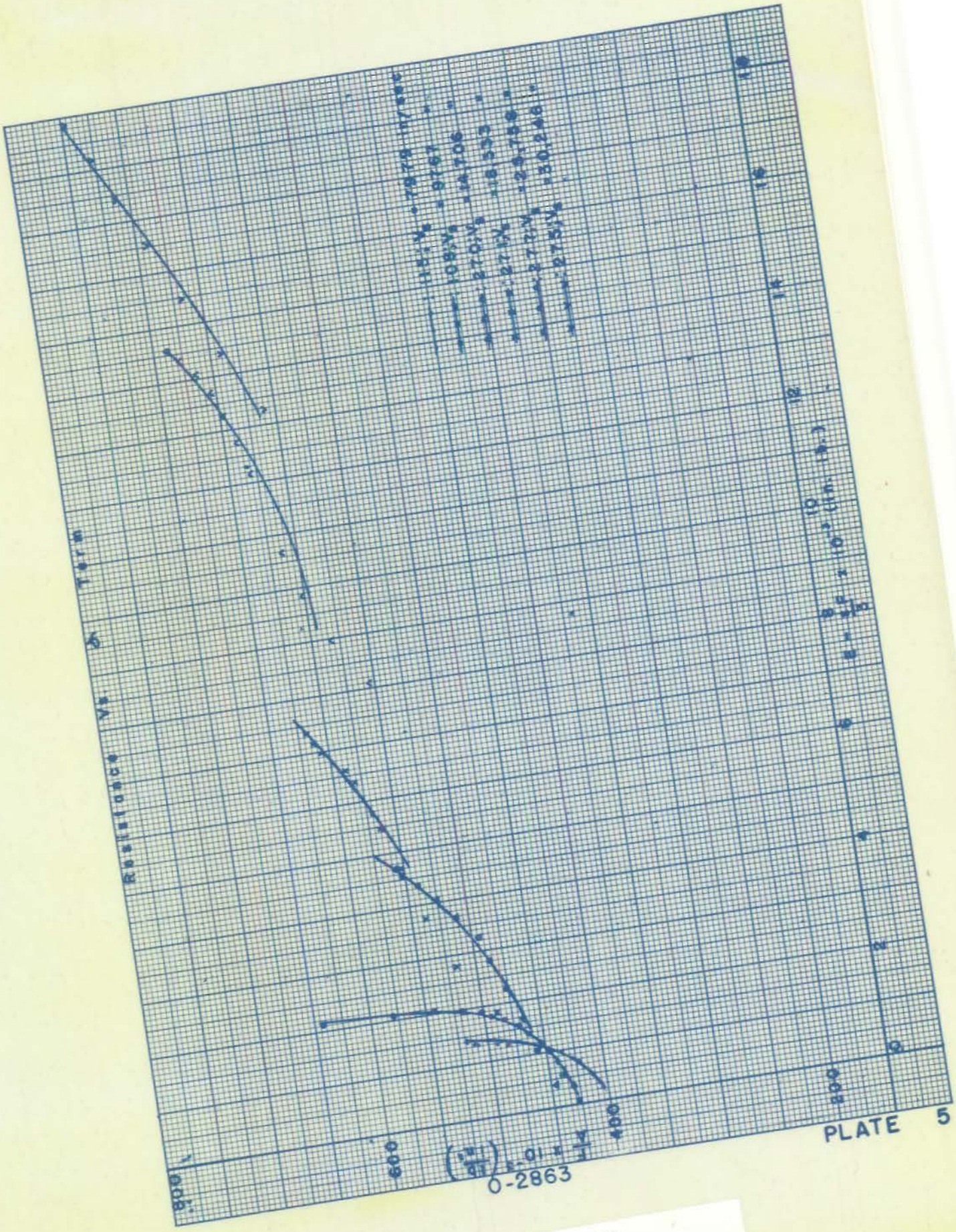

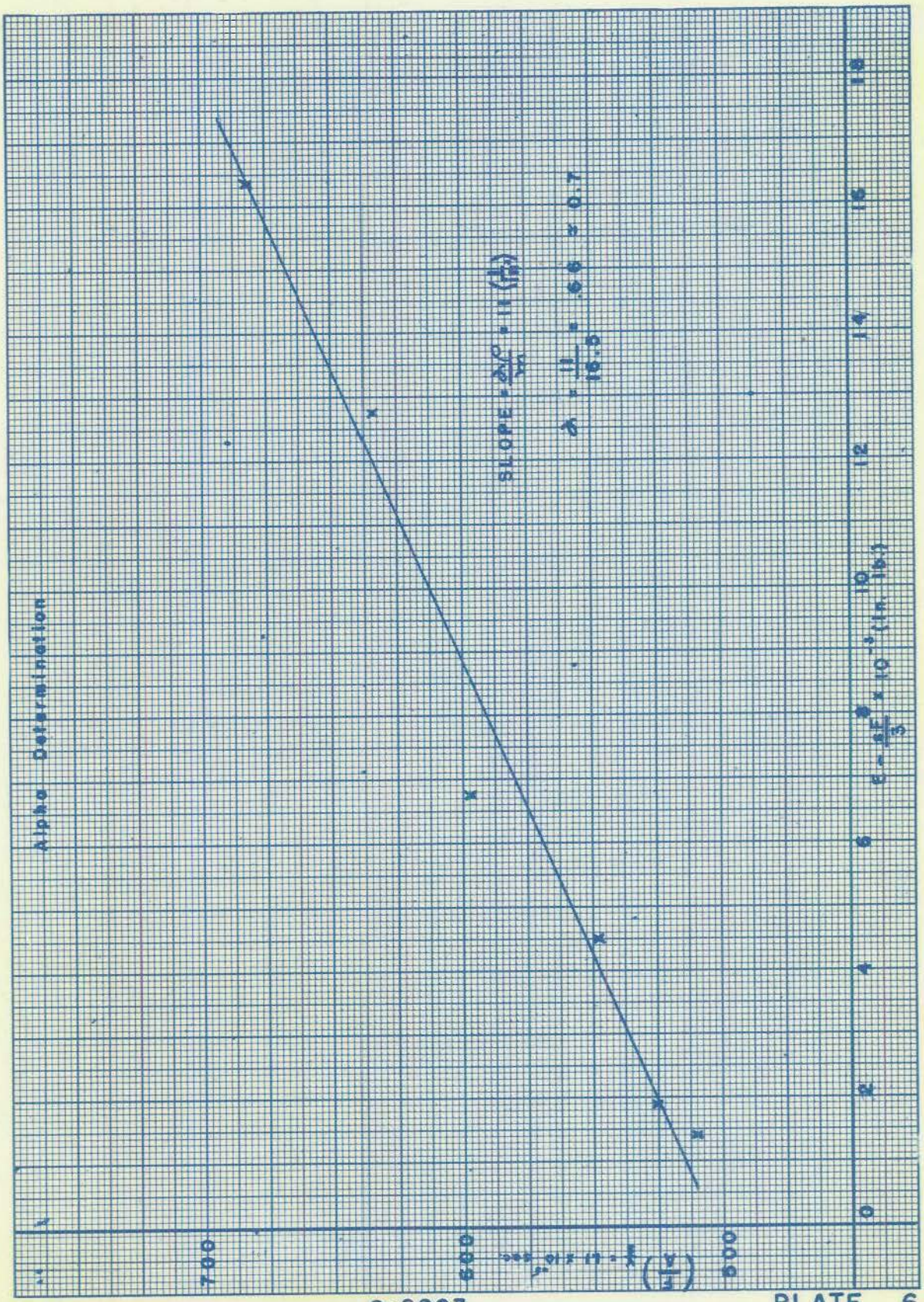

0-2863

PLATE 6

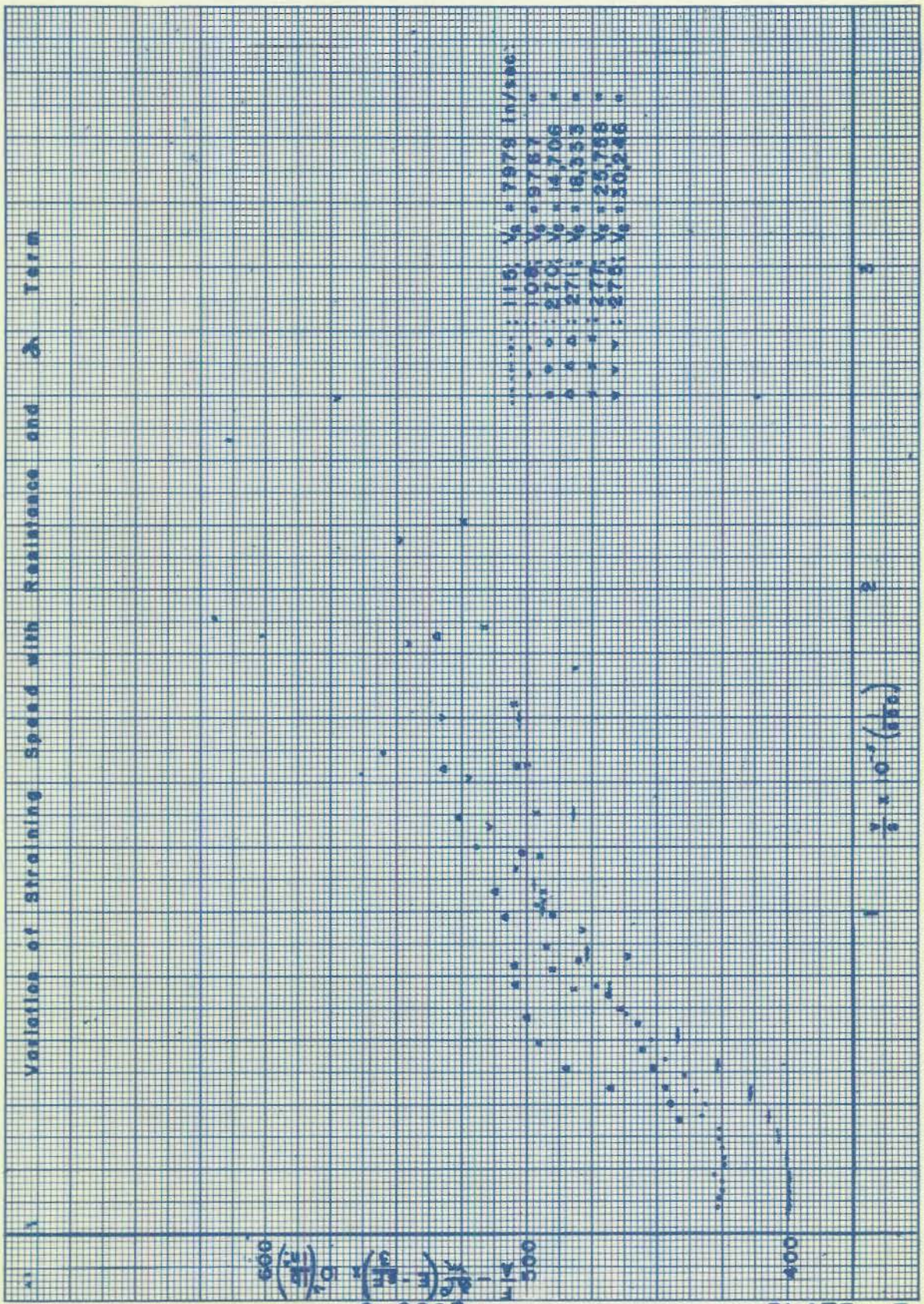

O-2863

PLATE 7

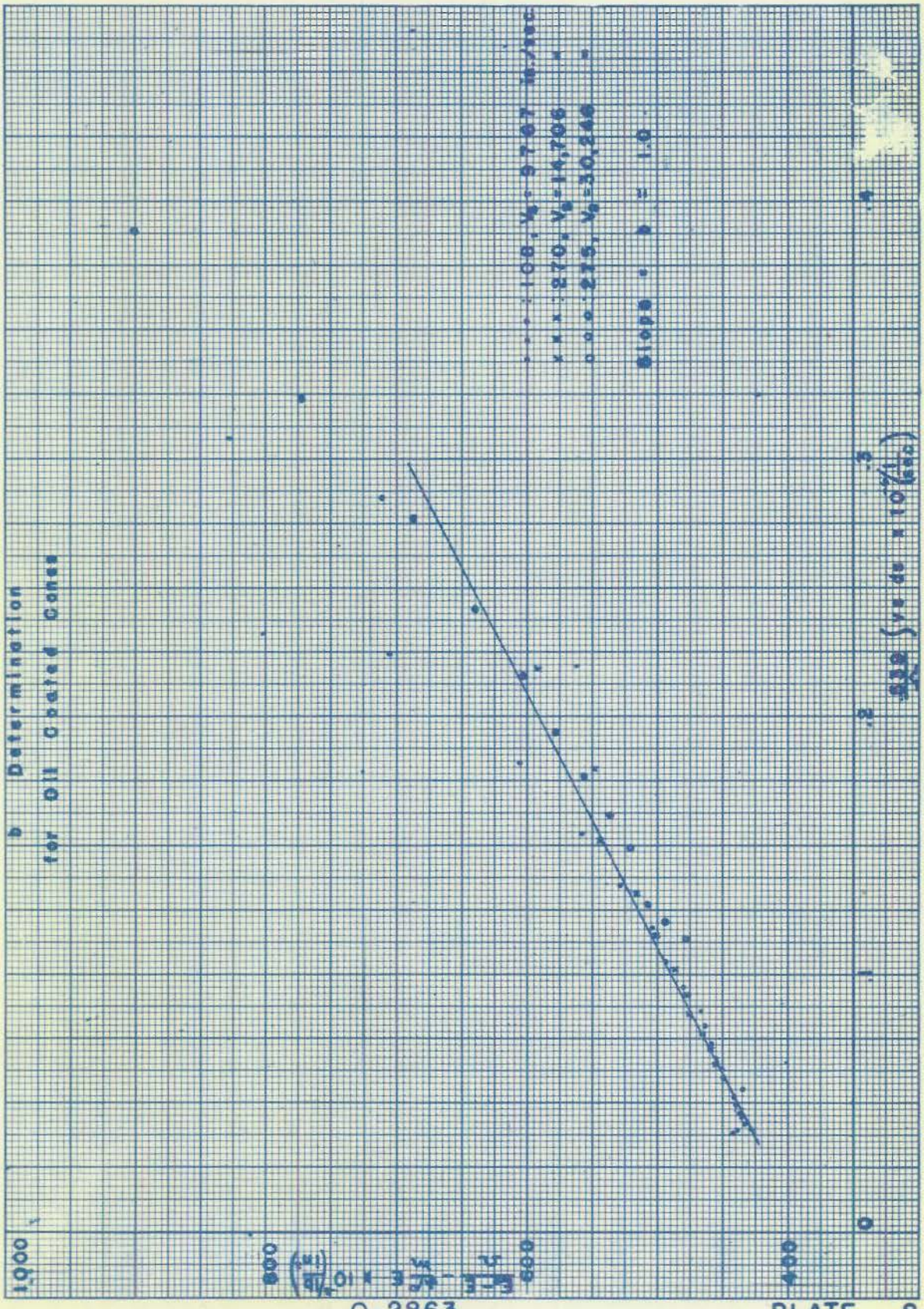

O-2863

PLATE 8

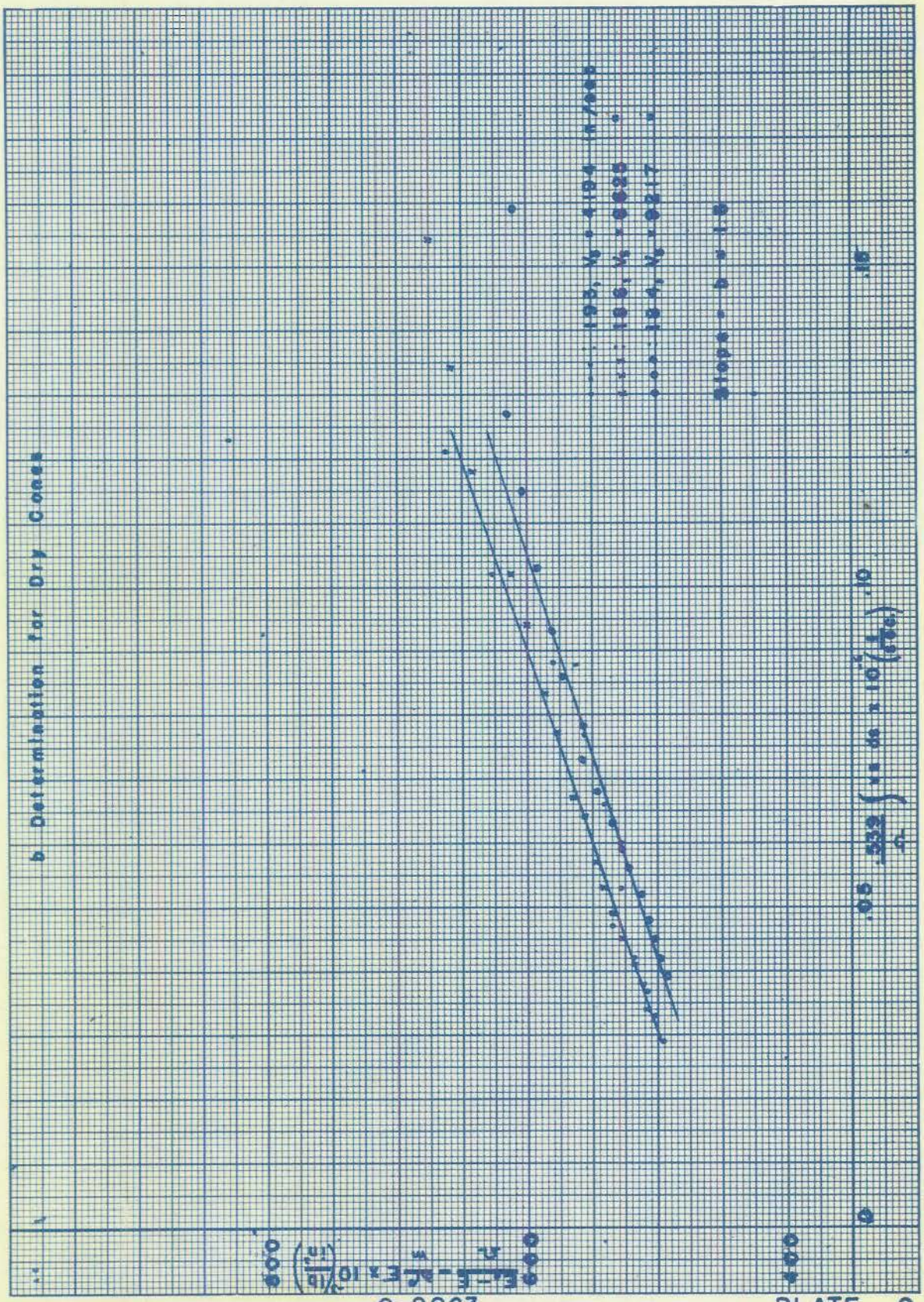

0-2863

PLATE 9

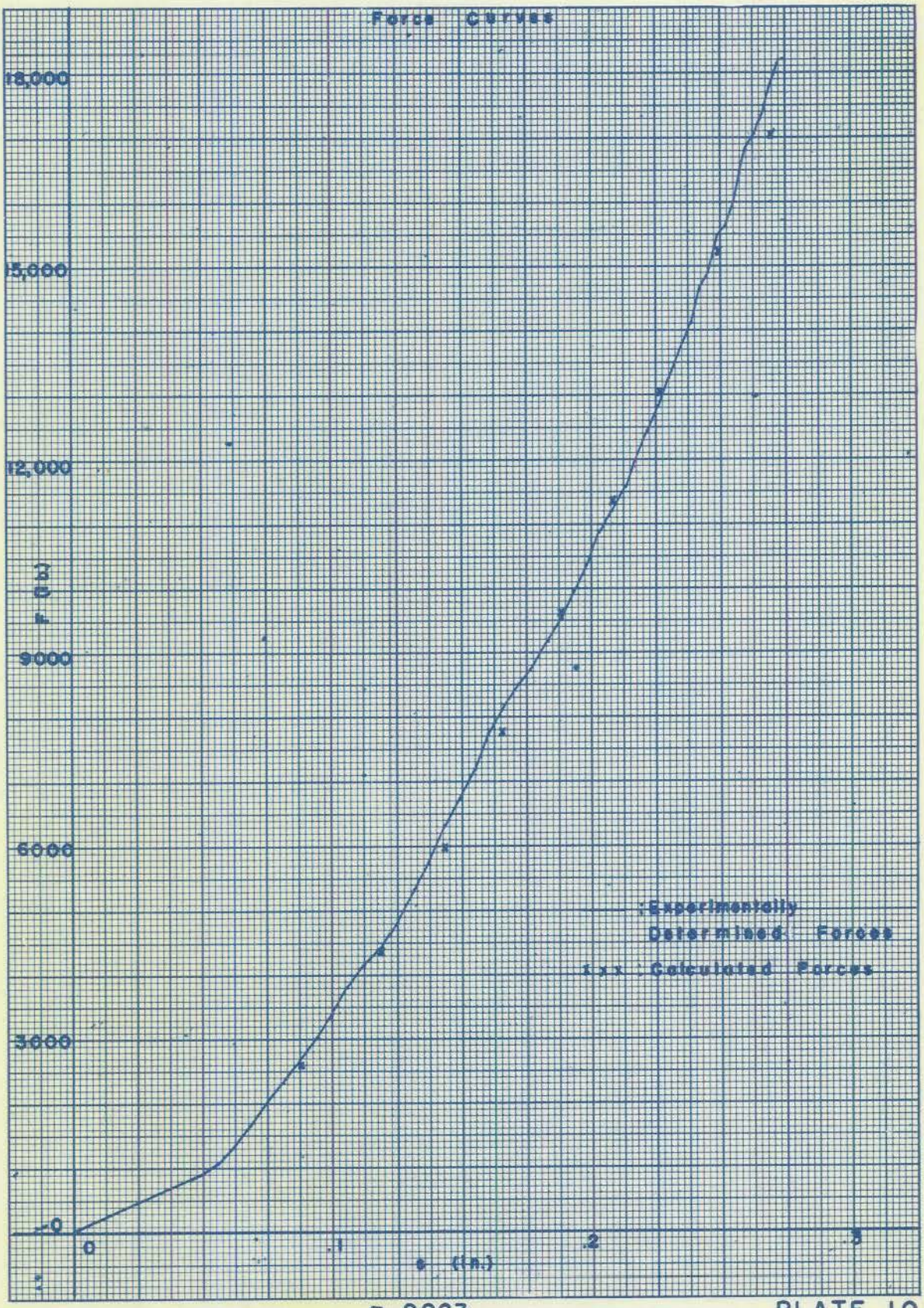

0-2863

PLATE 10

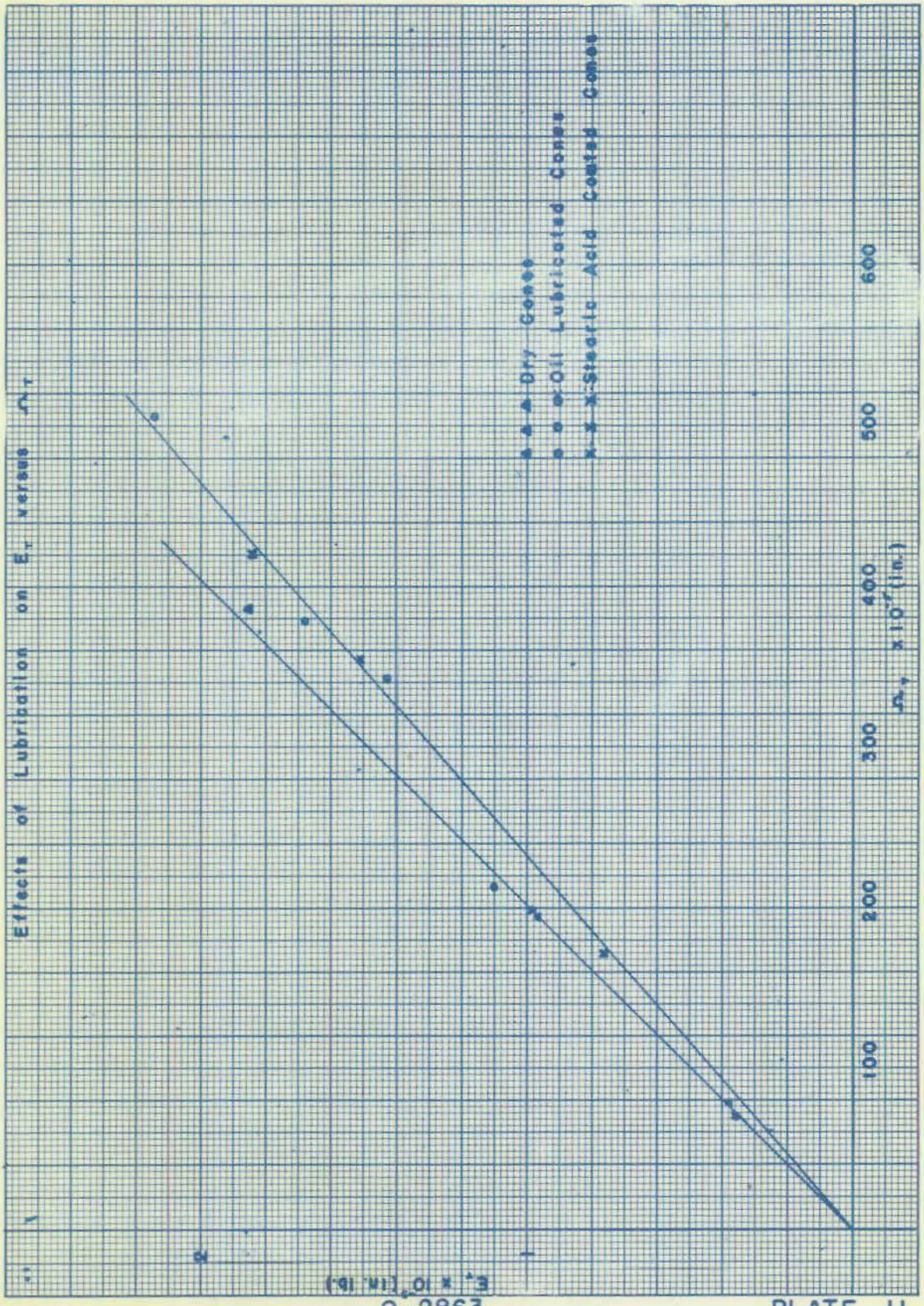

O-2863

PLATE 11